Possible Link of the V-Shaped Phase Diagram to the Glass-Forming Ability and Fragility in a Water-Salt Mixture

Mika Kobayashi and Hajime Tanaka*

Institute of Industrial Science, University of Tokyo, Meguro-ku, Tokyo 153-8505, Japan

(Received 10 November 2010; revised manuscript received 4 February 2011; published 25 March 2011)

Water is a very poor glass former, but its link to the thermodynamic and kinetic anomalies remains elusive. We experimentally reveal that the glass-forming ability and fragility of a water-salt mixture are closely related to its equilibrium phase diagram. We propose that frustration between local and global orderings controls both the glass-forming ability and the fragility. Relying on the same role of salt and pressure, which commonly break tetrahedral order, we apply this idea to pure water under pressure. This scenario not only explains unusual behavior of water-type liquids such as water, Si, and Ge but also provides a mechanism for a link between the equilibrium phase diagram, glass-forming ability, and fragility for various materials including oxides, chalcogenides, and metallic glasses.

DOI: 10.1103/PhysRevLett.106.125703 PACS numbers: 64.70.pm, 64.70.dg, 64.60.My

Water is known to exhibit a number of anomalous behaviors, compared to many other liquids [1–6]. They include the density maximum at 4 °C, the volume increase upon freezing into the ice crystal, the anomalous increase in the specific heat at constant pressure and the isothermal compressibility upon cooling, and the decrease of the viscosity with an increase in pressure (up to ~2 kbar). Furthermore, water is known as a very poor glass former, which is a significant drawback in the low-temperature storage of food and biomatter. Supercooled water so easily crystallizes into ice below its homogeneous nucleation temperature T_H, as monatomic liquids do. Recently, computer simulations started to provide key information on crystal nucleation in a supercooled water [7].

Despite the difficulty in vitrifying water, there are a few routes to the formation of amorphous ices [2–5,8]: depositing water vapor on a cold substrate or rapidly cooling emulsified water ($> 10^6$ K/s). It is also known that there exist more than two distinct forms of amorphous ices [2]. Low density and high density amorphous ice are well-known examples. High density amorphous ice is obtained by applying a high pressure to ice Ih at a low temperature. Low density amorphous ice can be obtained by releasing pressure applied to high density amorphous ice at a low temperature. This polyamorphism of water is suggestive of the existence of more than two liquid states [2,9], which yet needs to be confirmed.

For pure water, it is known that the anomalous behaviors of water and the glass-forming ability (GFA) are strongly influenced by pressure P [3,8,10,11]. Interestingly, it was shown that the addition of salt has the same effect as the increase of pressure: Both lead to the weakening of the anomalies. For example, Leberman and Soper compared the effects of salt and pressure, by using the intermolecular H-H pair correlation function of water, and found that both have the same effects on water structures [12]. Furthermore, Raman scattering studies showed that the addition of LiCl to water breaks tetrahedral structures stabilized by hydrogen bondings [13]. These indicate that both salt and pressure are breakers of local tetrahedral order [13,14]: It is local tetrahedral ordering that is a key to the water anomalies and GFA.

Here we experimentally study the GFA and the fragility [15] of a water-salt mixture as a function of the salt concentration. Based on experimental results, we suggest an intriguing scenario that there may be an intimate link of the shape of an ''equilibrium'' phase diagram to ''non-equilibrium'' glass transition behavior such as liquid fragility and glass-forming ability.

We used a water-LiCl mixture as a model system, following pioneering works of Angell and his co-workers (see, e.g., [16–18]). LiCl can be dissolved to exceptionally high salt concentrations in water, which allows us to investigate a wide range of the salt concentration. We prepared a sample, $LiCl \cdot RH_2O$, by mixing LiCl (99.8%, Wako Chemical) with water in a range of $R \geq 2.4$ (molar LiCl concentration: $\phi \leq 29.4\%$; mass LiCl concentration: $\leq 49.5\%$). Here R is the number of water molecules per LiCl molecule: Smaller R corresponds to higher ϕ. Differential scanning calorimetry (DSC) measurements were performed by a DSC instrument (Mettler Toledo, DSC822e), capable of both conventional (dc) and temperature-modulated (ac) measurements (TMDSC). Viscosity measurements were performed by using a rheometer (Reologica, DAR-100) with the cone plate geometry (diameter 25 mm and angle 4°).

First we show the phase diagram of water-LiCl mixtures in Fig. 1(a). There are two melting curves, which merge at $R_x = 6.5$ ($\phi_x \sim 13\%$) and thus have the minimum there. Here the melting point T_m was measured by conventional DSC measurements on heating at 5 K/min for a crystallized sample. It is known that in the region of $R > 6$ ice Ih precipitates and the rest of the sample remains disordered phase [19], whereas in the region of $R < 6$ hydrate crystals

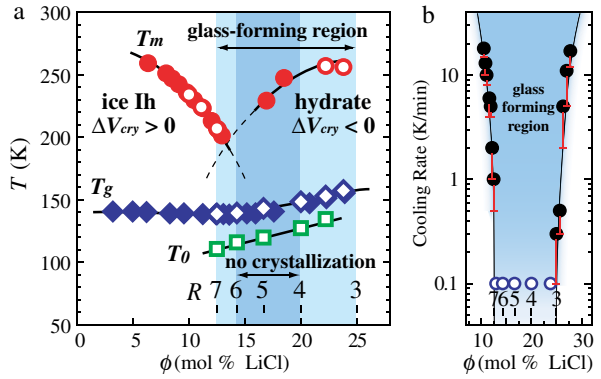

FIG. 1 (color online). (a) Phase diagram of water-LiCl mixtures. Red circles, T_m; blue diamonds, T_g; green squares, T_0. Closed symbols are taken from Ref. [39], which agree well with our data. (b) Critical cooling rate for vitrification, determined by DSC. Open circles means no sign of crystallization even for the slowest cooling rate (0.1 K/ min). Solid curves are guides to the eyes.

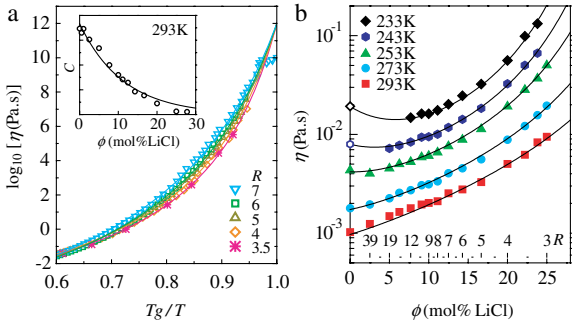

FIG. 3 (color online). (a) The Angell plot of η for LiCl · RH$_2$O: η vs T_g/T, where T_g is defined as a temperature where the viscosity extrapolated from the Vogel-Fulcher-Tammann relation becomes 10^{12} Pa · s. Solid curves are Vogel-Fulcher-Tammann fits to the data. Data were collected during cooling at 1 K/ min. The inset shows the ϕ dependence of the fraction of tetrahedral structures C estimated from Raman scattering measurements (see [32]). The curve is an exponential fit. (b) The ϕ dependence of η for several T's. The solid curves are fits to our prediction (see [32]).

of LiCl · RH$_2$O are formed. Figure 1(b) shows the critical cooling rate Q_c required for vitrification, i.e., a minimum cooling rate for which we do not observe any exothermic peak due to crystallization in DSC curves. We identify a good glass-forming region as $R = 3$–7, where a uniform glassy state is formed for a cooling rate $Q \leq 0.1$ K/ min. Particularly for $R = 4$–6, we never see any indication of crystallization throughout our experiments on both cooling and heating. Here we note that this R region is located slightly below $R_x \sim 6.5$ [see Fig. 1(a)]. The calorimetric T_g was measured by TMDSC on heating at 1 K/ min, and the obtained heat flow curves are shown in Fig. 2(a).

Next we show the temperature (T) dependence of shear viscosity η in Fig. 3(a). We analyze these data by fitting the Vogel-Fulcher-Tammann relation: $\eta = \eta_0 \exp[DT_0/(T - T_0)]$, where η_0, D, and T_0 are the fitting parameters.

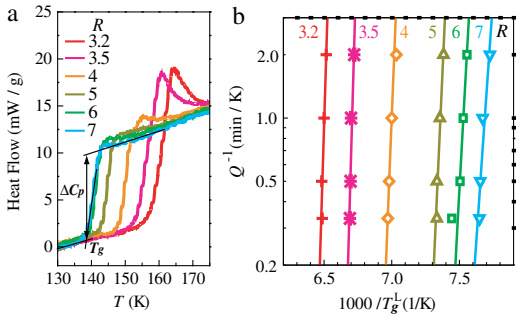

FIG. 2 (color online). (a) The reversible heat flow of LiCl · RH$_2$O measured by TMDSC (heating rate 1 K/ min, temperature modulation amplitude = 0.16 K, and the modulation frequency = 60 s). We set the signals at 130 K to be zero. (b) The inverse of the cooling rate Q plotted against the inverse of T_g^L determined by DSC measurements. The straight lines are results of linear fits. The slope becomes steeper with a decrease in R, indicating that the liquid becomes more fragile.

D is the so-called fragility index, but note that larger D means less fragile. T_0 is the ideal glass transition temperature, where η hypothetically diverges. The parameters D and T_0 obtained by the fittings are shown in Figs. 4(a) and 1(a), respectively. The decrease of D with an increase in ϕ indicates the increase in the fragility with ϕ.

We also estimate the fragility parameter m, which is defined as a slope of the T dependence of the relaxation time τ at T_g [20]: $m \equiv d[\log_{10}(\tau)]/d(T_g/T)|_{T=T_g}$. Note that larger m means more fragile. To directly estimate m, we measured the Q dependence of T_g^L, which is the low-temperature edge of a step associated with the glass transition upon cooling in a DSC signal [21] [see Fig. 2(b)]. From the above definition of m, we estimated the values of m, which are shown in Fig. 4(a). For comparison, we also estimated the values of m from our viscosity measurements, by using the following relation between m and D: $m = (D/\ln 10)(T_0/T_g)[1 - (T_0/T_g)]^{-2}$. As shown in

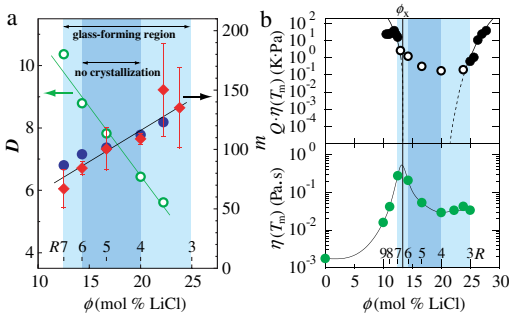

FIG. 4 (color online). (a) ϕ (or R) dependence of D (open circles) and m. Diamonds are m estimated from DSC [see Fig. 2 (b)], whereas filled circles are m converted from D (see the text). Solid lines are guides to the eyes. (b) Bottom: Dependence of η at T_m as a function of ϕ ($\eta[T_m(\phi)]$). Top: ϕ dependence of $Q\eta$.

Fig. 4(a), the value m estimated from DSC very well agrees with that from viscosity measurements.

Next we consider the GFA. The ϕ dependence of η at $T_m(\phi)$ is shown in Fig. 4(b). Reflecting the lower T_m near the triple point, η has a maximum near ϕ_x ($R_x \sim 6.5$). However, this kinetic factor alone cannot explain the steep minimum of Q_c around $R = 4$–5 [see Fig. 1(b)]. This is evident from the very deep minimum in $Q\eta$ near ϕ_X shown in Fig. 4(b). This indicates the importance of a thermodynamic factor, i.e., the energetic frustration.

Now we discuss the above results in the light of our two-order-parameter model of liquid, which focuses on local structural ordering in a liquid [22,23]. We assume that locally favored structures [low-entropy, ordered states (LFS)] are created and annihilated in a sea of normal-liquid structures (high-entropy, disordered states). This simple two-state model well explains the thermodynamic and kinetic anomalies of water [24–27]. Here we note that for water both normal-liquid structures and LFS are dominated by hydrogen bonding but with less tetrahedrality for the former (see, e.g., [24,27]). In usual liquids, an equilibrium crystal is stabilized mainly by intermolecular attractions, and thus the density increases upon crystallization (i.e., the volume change upon crystallization $\Delta V_{\rm cry} < 0$). We refer this type of crystallization to density (ρ) ordering and the resulting crystal to ρ crystal. On the other hand, LFS is usually stabilized by directional bonding (hydrogen bonding for molecular liquids or covalent bonding for atomic liquids), and we refer this type of ordering to bond (S) ordering. Based on this picture, the origin of vitrification can be explained as follows [22,23]. When the symmetry of LFS is not consistent with that of the equilibrium ρ crystal, which is a result of ''global'' minimization of the free energy, LFS acts as a source of frustration, or impurity, against crystallization. This competition between the two types of ordering, local vs global, should help a liquid to bypass crystallization and vitrify [22,23]. Thus, the increase in the degree of frustration is expected to increase the GFA, which was recently confirmed by numerical simulations [28,29].

In some exceptional cases, however, a system can attain global bond ordering or form a crystal stabilized by directional bonding, i.e., S crystal. This is the case of water [24,26]: The structure of ice Ih is consistent with the tetrahedral structure of water LFS. This means that for water at ambient pressure crystallization can be regarded as global S ordering and thus LFS helps crystallization rather than interferes it. The volume expansion upon crystallization ($\Delta V_{\rm cry} > 0$) is a consequence of S ordering toward tetrahedrality. This explains the very poor GFA of pure water at ambient pressure.

However, this situation changes with an increase in pressure (Fig. 5) [26]. Under high pressure, bulky tetrahedral order is not favored. The crystal structure changes from hexagonal ice Ih to tetragonal ice III at a critical pressure P_x (~ 2 kbar) (the triple point), where the two

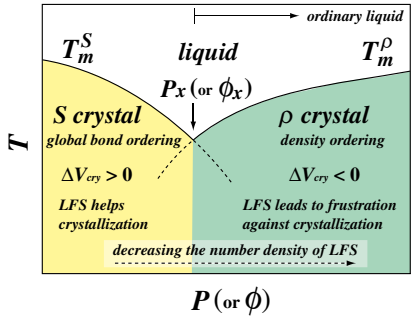

FIG. 5 (color online). Schematic P-T phase diagram of water-type liquids. The axis P can be replaced by the concentration ϕ of a destabilizer of S order (LFS).

melting curves merge and T_m has a minimum. This leads to the density increase of the crystal from 0.92 to 1.14 across P_x [30], which results in $\Delta V_{\rm cry} < 0$ above P_x. We may say that the crystal structure changes from S crystal to ρ crystal at P_x. According to our scenario [24,26,31], water should behave as an ordinary liquid above P_x and the GFA should increase there, which was supported by the decrease of Q_c for vitrification by about 3 orders of magnitude around a few kbar [11,32] than at ambient pressure [33]. The increase of the GFA of water at high pressure was also reported in Refs. [8,10,34]. We stress that this cannot be explained by a kinetic factor (viscosity increase) alone.

In our model, the fragility of a liquid is determined by the degree of frustration between LFS and crystallization. Stronger frustration leads to a larger distance between the onset temperature of cooperativity (near T_m) and T_0, where the relaxation time hypothetically diverges [22,23,28]. This larger T_m-T_0 means a slower (more Arrhenius-like) increase in η upon cooling, i.e., a stronger liquid. For pure deuterated water, Lang and Lüdemann [10] reported that the fragility index D is 4.6, 4.3, and 3.9, respectively, for $P = 1.5$, 2.0, and 2.5 kbar. This suggests that water becomes more fragile with an increase in P, or with a decrease in S, consistent with our scenario.

Let us return to the case of water-LiCl mixtures. $\Delta V_{\rm cry} > 0$ for $R = 8.56$ (density measurements [35]), whereas $\Delta V_{\rm cry} < 0$ for $R = 3$ (our eye inspection). This implies that $\Delta V_{\rm cry}$ changes its sign from positive to negative with an increase in ϕ, supporting the existence of a change in the stable crystal structure from S crystal to ρ crystal [see Figs. 1(a) and 5].

We also confirmed the decrease of the fraction of LFS, C, with an increase in ϕ by both Raman scattering measurements [the inset in Fig. 3(a)] and the ϕ dependence of η [Fig. 3(b)] (see [32] for the details). This clearly shows that the increase in ϕ decreases LFS, as the increase in pressure does for pure water.

Thus, at low ϕ (i.e., at large R), the situation is similar to that of pure water at ambient pressure. Ice Ih is easily formed due to its consistency with the tetrahedral structure of LFS: very poor GFA. For a concentration near and above ϕ_x, LFS finally becomes incompatible with the

equilibrium crystal structure, which is "$LiCl \cdot RH_2O$ crystal." This situation for $\phi > \phi_x$ is similar to ordinary liquids with $\Delta V_{cry} < 0$. In this region, an increase in ϕ leads to further breaking of tetrahedral LFSs, which decreases the degree of frustration on the formation of ρ crystal. This should result in the decrease in the GFA and the increase in the fragility, which explains our results [see Figs. 1(a) and 4(a)].

In sum, we experimentally established an intimate link of the shape of the equilibrium phase diagram [Fig. 1(a)] to the GFA [Fig. 1(b)] and the fragility [Fig. 4(a)]. Our finding suggests a thermodynamic origin of glass transition. Such a link was predicted theoretically [31] and then supported by simulations [28,36] and an experimental study on the glass formation near the triple point for Ge [37]. What is new here is experimental evidence for systematic changes in both the GFA and the fragility of a liquid near the triple point. This provides a possibility to predict the GFA and fragility from the shape of the equilibrium phase diagram. The key is the relationship between global minimization of the free energy toward crystal and local minimization toward LFS. Depending upon the consistency of these two symmetries, LFS can be either a promoter of crystallization or its preventer. Surprisingly, the ϕ dependence of the GFA is much stronger than that of the fragility. This suggests that the frustration has more drastic effects on the thermodynamic factor than the kinetic factor, which needs to be explained in the future. A physical factor making water so unusual among "molecular" liquids is the V-shaped P-T phase diagram: Water may be only such a molecule. Our scenario can be applied not only to pure water but also to other water-type liquids [31] such as Si and Ge [36,37], which also have V-shaped P-T phase diagrams. Instead of changing pressure, we can add additives to a liquid to modify the number density of LFS, which opens up a new possibility to control the GFA and the fragility of a liquid in a systematic way. Typical examples are salt for water, Na_2O for SiO_2 [16], and Au for Si [38]. Our finding may shed new light on a general mechanism of glass transition.

The authors thank C. A. Angell, G. Floudas, and Y. Suzuki for valuable discussions and also A. Kaltbeitzel, P. Räder, and D. Vollmer for technical supports for DSC measurements. This work was partially supported by a grant-in-aid from the Ministry of Education, Culture, Sports, Science and Technology, Japan.

*tanaka@iis.u-tokyo.ac.jp

[1] D. Eisenberg and W. Kauzmann, *The Structure and Properties of Water* (Oxford University, New York, 1969).
[2] O. Mishima and H. E. Stanley, Nature (London) **396**, 329 (1998).
[3] P. G. Debenedetti, J. Phys. Condens. Matter **15**, R1669 (2003).
[4] T. Loerting and N. Giovambattista, J. Phys. Condens. Matter **18**, R919 (2006).
[5] C. A. Angell, Science **319**, 582 (2008).
[6] A. K. Soper, Mol. Phys. **106**, 2053 (2008).
[7] M. Matsumoto, S. Saito, and I. Ohmine, Nature (London) **416**, 409 (2002); M. Yamada *et al.*, Phys. Rev. Lett. **88**, 195701 (2002); R. Radhakrishnan and B. L. Trout, Phys. Rev. Lett. **90**, 158301 (2003); E. B. Moore and V. Molinero, J. Chem. Phys. **132**, 244504 (2010).
[8] C. A. Angell, Annu. Rev. Phys. Chem. **55**, 559 (2004).
[9] P. H. Poole *et al.*, Nature (London) **360**, 324 (1992).
[10] E. W. Lang and H.-D. Lüdemann, Angew. Chem., Int. Ed. Engl. **21**, 315 (1982).
[11] O. Mishima and Y. Suzuki, J. Chem. Phys. **115**, 4199 (2001).
[12] R. Leberman and A. K. Soper, Nature (London) **378**, 364 (1995).
[13] J. L. Green, A. R. Lacey, and M. G. Sceats, Chem. Phys. Lett. **134**, 385 (1987).
[14] F. H. Stillinger and A. Ben-Naim, J. Phys. Chem. **73**, 900 (1969).
[15] Here the fragility is a measure of how steeply the viscosity increases toward T_g. Liquids with a super-Arrhenius temperature dependence of viscosity η are called "fragile," whereas those with an Arrhenius one are called "strong."
[16] C. A. Angell and E. J. Sare, J. Chem. Phys. **49**, 4713 (1968).
[17] C. A. Angell *et al.*, J. Food Eng. **22**, 115 (1994).
[18] C. A. Angell, Chem. Rev. **102**, 2627 (2002).
[19] A. Elarby-Aouizerat *et al.*, J. Non-Cryst. Solids **104**, 203 (1988).
[20] R. Böhmer and C. A. Angell, Phys. Rev. B **45**, 10 091 (1992).
[21] C. T. Moynihan *et al.*, J. Phys. Chem. **78**, 2673 (1974).
[22] H. Tanaka, J. Phys. Condens. Matter **10**, L207 (1998).
[23] H. Tanaka, J. Chem. Phys. **111**, 3163 (1999).
[24] H. Tanaka, Europhys. Lett. **50**, 340 (2000).
[25] H. Tanaka, J. Chem. Phys. **112**, 799 (2000).
[26] H. Tanaka, J. Phys. Condens. Matter **15**, L703 (2003).
[27] G. A. Appignanesi, J. A. Rodriguez Fris, and F. Sciortino, Eur. Phys. J. E **29**, 305 (2009).
[28] H. Shintani and H. Tanaka, Nature Phys. **2**, 200 (2006).
[29] T. Kawasaki, T. Araki, and H. Tanaka, Phys. Rev. Lett. **99**, 215701 (2007).
[30] B. Kamb, Science **150**, 205 (1965).
[31] H. Tanaka, Phys. Rev. B **66**, 064202 (2002).
[32] See supplemental material at http://link.aps.org/supplemental/10.1103/PhysRevLett.106.125703 for information on various types of amorphous water, salt-induced breakage of tetrahedral structures, and pressure effects on the GFA and fragility of water.
[33] P. Brüggeller and E. Mayer, Nature (London) **288**, 569 (1980).
[34] N. Sartori, K. Richter, and J. Dubochet, J. Microsc. **172**, 55 (1993).
[35] J. Fornazero, A. El Hachadi, and J. Dupuy-Philon, J. Non-Cryst. Solids **150**, 413 (1992).
[36] V. Molinero, S. Sastry, and C. A. Angell, Phys. Rev. Lett. **97**, 075701 (2006).
[37] M. H. Bhat *et al.*, Nature (London) **448**, 787 (2007).
[38] A. Pasturel *et al.*, Phys. Rev. B **81**, 140202(R) (2010).
[39] B. Prével *et al.*, J. Chem. Phys. **103**, 1886 (1995).